Enhanced Molecular Orientation and Strain Hardening in Melt-Spun Isotactic Polypropylene Monofilaments Through Partial Melting Recrystallization

Zhujun Li, Bing Na, Nana Tian, Ruihua Lv, Shufen Zou

Department of Materials Science and Engineering, Key Laboratory of Radioactive Geology and Exploration Technology Fundamental Science for National Defense, School of Biology, Chemistry and Material Science, East China Institute of Technology, Fuzhou, 344000, People's Republic of China

Received 26 July 2010; accepted 22 March 2011
DOI 10.1002/app.34541
Published online 9 August 2011 in Wiley Online Library (wileyonlinelibrary.com).

ABSTRACT: Achieving high molecular orientation, by increasing spinning velocity and/or postdrawing, is critical to improve the mechanical properties of isotactic polypropylene (iPP) fibers. In this study, we have demonstrated that upon annealing around melting point the molecular orientation of both amorphous and crystalline phases in melt-spun iPP monofilaments is significantly enhanced, in parallel with the improved stability of crystals, because of partial melting and oriented recrystallization. As a result, high level stress and remarkable strain hardening are generated during stretching of annealed monofilaments. © 2011 Wiley Periodicals, Inc. J Appl Polym Sci 123: 995–999, 2012

Key words: molecular orientation; strain hardening; partial melting recrystallization

INTRODUCTION

During melt spinning flow-induced molecular orientation and crystallization are common observations for isotactic polypropylene (iPP) fibers, which depends on the melt temperature, take-up velocity, molecular weight, molecular weight distribution, and so forth.[1–4] It is believed that the formation of oriented morphology during flow involves two stages: the aligned chains are first transformed into shish structures as primary nuclei, followed by the transverse growth of folded chain lamellae, kebabs, on them.[5,6] Upon reheating the shish structure in the oriented iPP can survive even above nominal melting temperature, and shows higher thermal stability than its kebab counterpart.[7,8]

The extent of molecular orientation in the iPP fibers dictates the mechanical properties to a large extent. Hence, in practice achieving high molecular orientation through increasing spinning velocity and/or postdrawing of as-spun fibers is critical to obtain superior mechanical properties.[1,9–11] In a general scheme, the development of molecular orientation and mechanical properties in the final fibers is understood in term of the stretching of a molecular network with crystallites acting as network junctions.[1,12,13] On the contrary, annealing of iPP fibers at temperatures where α-process is activated could give rise to local relaxation of oriented strands and thus the decreased molecular orientation in the amorphous phase,[14] accompanied by the structural rearrangements in the crystalline regions. This could alter the molecular network and thus affect the mechanical responses in the annealed iPP filaments.[15–17] In the past studies, the annealing temperature is usually below the melting temperature of iPP, and the structural changes around melting point and their influences on the mechanical responses are little concerned.

In this study, annealing of melt-spun iPP monofilaments with fixed ends has been conducted at 165°C. Enhanced molecular orientation, as revealed by two dimensional wide angle X-ray diffraction (2D-WAXD) and infrared microscopy (micro-FTIR) measurements, has been achieved due to partial melting and oriented recrystallization. Moreover, outstanding mechanical response at large strain, that is, strain hardening, is presented in the annealed iPP monofilaments, because of the combined effects of increased molecular orientation and improved stability of crystals.

Correspondence to: B. Na (bingnash@163.com or bna@ecit.edu.cn).

Contract grant sponsor: The National Natural Science Foundation of China; contract grant number: 20704006.
Contract grant sponsor: The Project of Jiangxi Provincial Department of Education; contract grant number: GJJ08295.
Contract grant sponsor: The Opening Project of the State Key Laboratory of Polymer Materials Engineering, Sichuan University.

EXPERIMENTAL

Material and sample preparation

A commercial iPP homopolymer, supplied by Yanshan Petroleum (China) was used. It had Mw of 39.9 × 10^4 g/mol, Mw/Mn of 4.6, and melting point of about 165°C, respectively. A modified capillary rheometer, operated at constant extrusion speed of 3 mm/min, was adopted to produce iPP monofilaments at a melt temperature of 200°C. The extruded melt was transformed into solid monofilaments with a diameter of about 60 μm at a take-up velocity of about 80 m/min under air-cooling. To prepare annealed ones, as-spun monofilaments were first fixed on a glass plate with clips at two ends and then annealed for 15 min in an oven at 165°C. Note that at this high temperature partial melting of as-spun monofilaments is expected and recrystallization could occur upon cooling to room temperature.

Structural characterizations

Differential scanning calorimetry

The melting behaviors of as-spun and annealed iPP monofilaments with mass of about 7 mg were registered at a heating rate of 10°C/min in a nitrogen atmosphere using a NETZSCH DSC 204.

Two dimensional wide angle X-ray diffraction

2D-WAXD measurements on a bundle of monofilaments were conducted on the diffraction workstation in the National Synchrotron Radiation Laboratory (Hefei, China). The wavelength of X-ray was 0.154 nm and the exposure time was 5 min.

Two dimensional small angle X-ray scattering

2D-SAXS measurements on a bundle of monofilaments were conducted on a Bruker Nanostar small angle scattering set-up. The wavelength of X-ray was 0.154 nm, and the SAXS data were subtracted from background scattering.

Video-aid tensile tests

Mechanical tests of a monofilament were performed on a universal testing machine at room temperature with a crosshead speed of 5 mm/min. Prior to tests the diameter of each monofilament was precisely measured by an optical microscope with resolution of 2 pixels per micron. A CCD camera (1280 pixel ×1024 pixel), equipped with a tunable magnification lens, was adopted to monitor the longitudinal separation of inkmarks preprinted on the surface of monofilaments during stretching. Reliable strain ε, defined as $\varepsilon = l/l_0 - 1$ (l and l_0 was the transient and initial length between two inkmarks, respectively), could be obtained through this procedure.

Micro-FTIR study of stretching

The structural evolutions during stretching of a monofilament were monitored by a Thermo Nicolet infrared microscope with a MCT detector coupled with a mini-stretcher at room temperature. The IR source was provided by a Thermo Nicolet FTIR spectrometer. During measurements the monofilament was stretched step by step at a rate of 5 mm/min along the fiber axis. The strain was precisely deduced from the extension of an inkmark preprinted on the monofilament. At each strain polarized infrared spectra (by rotating a ZnSe polarizer), parallel and perpendicular to the fiber axis, respectively, were collected with a resolution of 4 cm^{-1} and a total of 32 scans was added. Note that the microsampling position was the same for each strain, which was readily realized by moving the sample stage under a CCD view system of the IR microscope.

The order parameter f and structural absorbance A of a desired absorption band were deduced using following relations.[18]

$$f = [(R-1)(R_0+2)]/[(R+2)(R_0-1)] \quad (1)$$

$$R = A_{//}/A_{\perp},\ R_0 = 2\cot^2\alpha \quad (2)$$

$$A = (A_{//} + 2A_{\perp})/3 \quad (3)$$

where $A_{//}$ and $A_{\perp}$ was the parallel and perpendicular absorbance, respectively, and α was the angle between the dipole moment vector and the local chain axis. We emphasize that order parameter f assumes values from −0.5 to 1 (−0.5 for perfect molecular alignment perpendicular to the fiber axis, 0 for random orientation, and 1 for perfect molecular alignment along the fiber axis).

RESULTS AND DISCUSSION

Figure 1 shows the melting behaviors of as-spun and annealed iPP monofilaments. As compared with as-spun counterparts, the melting point in the annealed monofilaments shifts to higher temperature. It means that some imperfect crystals formed during melt spinning have been melted and recrystallized into more stable ones upon annealing at 165°C.

Figure 2 is the 2D-WAXD results recorded from as-spun and annealed monofilaments. From the patterns [Fig. 2(a,b)] two points can be made. First, only α-crystals of iPP, having characteristic reflection peaks of, (110), (040), and (130) planes, are presented in both types of monofilaments. Second, the

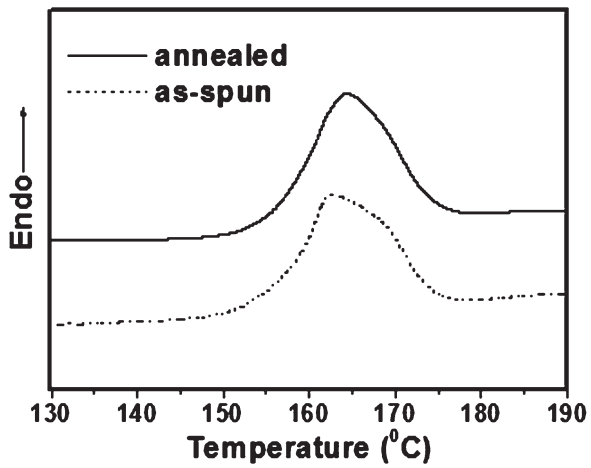

Figure 1 Melting traces of as-spun and annealed iPP monofilaments.

concentrated reflections at the equator of the (hk0) planes suggests apparent *c*-axis orientation in these monofilaments. Of note, *a*′-axis orientation, indicated by the off-meridianal reflections of (110) plane, arises from the lamellar branching through homoepitaxy between α-crystals of iPP.[16,19] This *a*′-axis orientation becomes significant in the as-spun monofilaments but almost disappears in the annealed ones. Furthermore, annealing-enhanced molecular orientation of crystalline phase can also be deduced, demonstrated by lower value of the full width at half-maximum (FWHM) of the azimuthally integrated peak intensity in the annealed monofilaments. As shown in Figure 2(c), the FWHM of (110) plane around equator is 9.6 and 6.4° for as-spun and annealed monofilaments, respectively. The unexpected increasing of molecular orientation strongly suggests that during annealing some unstable crystals with low *c*-axis orientation also endure melting, in addition to the destruction of the crystals with *a*′-axis orientation.

Therefore, it is believed that re-crystallization, nucleated by the surviving oriented crystals with high thermal stability, occurs in the annealed monofilaments. This situation is similar to that observed in the so-called "all-iPP" composites where highly oriented iPP fibers can withstand melting and induce interfacial crystallization of molten iPP matrix on them.[20–23] Moreover, 2D-SAXS results shown in Figure 3 indicate that recrystallization gives rise to the formation of regularly stacked lamellae and amorphous regions along fiber axis. Herein, two concentrated scattering spots along fiber axis are exhibited in the annealed monofilaments, whereas only diffuse scattering is presented in the as-spun ones [see Fig. 3(a,b)]. It is further verified by the scattering profile integrated from the patterns, as shown in Figure 3(c). A scattering peak is observed in the annealed monofilaments but absent in the as-spun counterparts.

However, recrystallization upon annealing also alters the molecular orientation in the amorphous phase of iPP monofilaments, as disclosed by the micro-FTIR results in Figure 4. The 998 cm^{-1} band corresponds to the crystalline phase, whereas the 974 cm^{-1} band is contributed by both the amorphous and crystalline phases.[24,25] Therefore, using eqs. (1) and (2) the molecular orientation of crystalline phase (f_c) and the average orientation (f_{av}) can be quantitatively determined from theses two bands with $\alpha = 18°$, respectively. Furthermore, the molecular orientation in the amorphous phase, f_a, is deduced by eqs. (4) and (5).[25]

$$f_a = (f_{av} - X_c f_c)/(1 - X_c) \quad (4)$$

$$X_c = 0.56A_{998}/A_{973} \quad (5)$$

It is indicated that the molecular orientation in both crystalline and amorphous phases is enhanced in the annealed monofilaments, as compared with those exhibited by the as-spun ones. In combination with above 2D-WAXD results, it means that oriented

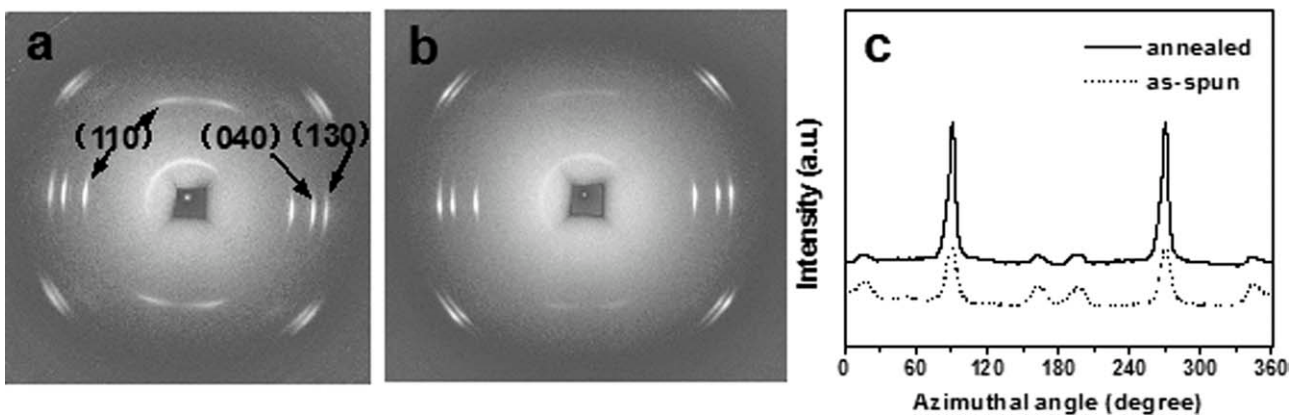

Figure 2 2D-WAXD patterns (a: as-spun; b: annealed) and azimuthal profiles of (110) plane (c) of iPP monofilaments. The fiber axis is nearly vertical.

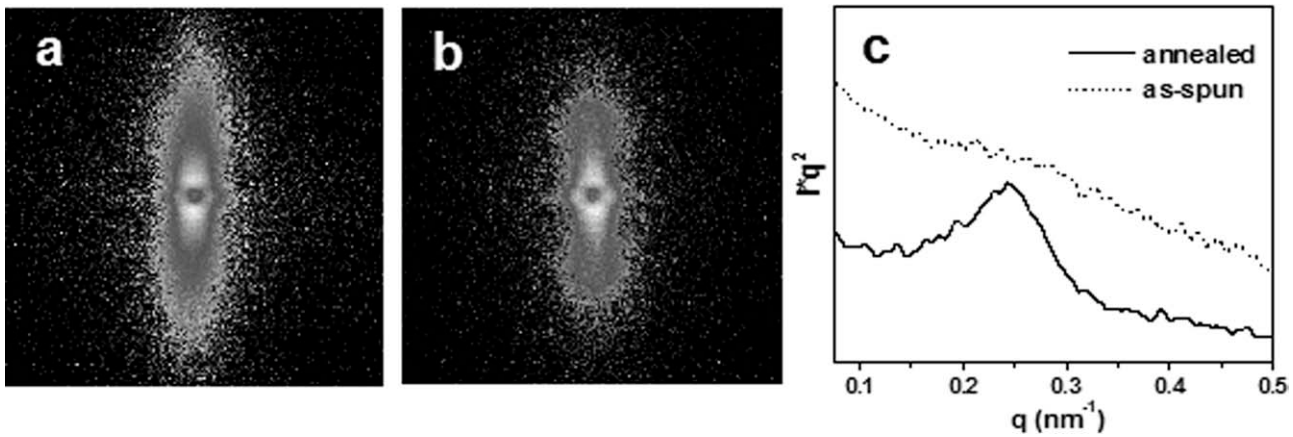

Figure 3 2D-SAXS patterns (a: as-spun; b: annealed) and scattering profiles (c) of iPP monofilaments. The fiber axis is nearly vertical.

recrystallization during annealing also results in local reorientation of amorphous strands located between adjacent lamellae, in line with other observation.[26]

Figure 5 is the typical stress-stain curves obtained from stretching of as-spun and annealed monofilaments. Beyond yield point significant strain hardening is presented in the annealed monofilaments, whereas stretching of as-spun ones only gives rise to the gradual increase in the stress level. According to numerous studies,[24,27–31] strain hardening at large strain of semicrystalline polymers results from the extension of amorphous strands in the molecular network with crystallites acting as physical cross-links. The higher the initial molecular orientation in the amorphous phase, the more significant strain hardening is expected during deformation. It is the fact observed for the stretching of annealed monofilaments with high initial molecular orientation. However, high stress generated by the amorphous molecular network also results from the enhanced stability of crystals that serve as network junctions in the annealed monofilaments.[28–31] Once the destruction of crystals sets in, further deformation is mainly accommodated by crystals rather than amorphous phase.[32] As a result, the extension and molecular orientation of amorphous strands could reach their limits.

To identify this, micro-FTIR studies of stretching of a monofilament has been carried out and the related results are complied in Figure 6. During stretching, the molecular orientation of amorphous phase in the annealed monofilaments first increases beyond yielding point, because of chain extension and then reaches a plateau at a strain of about 1.0. Rather, only gradual increase of molecular

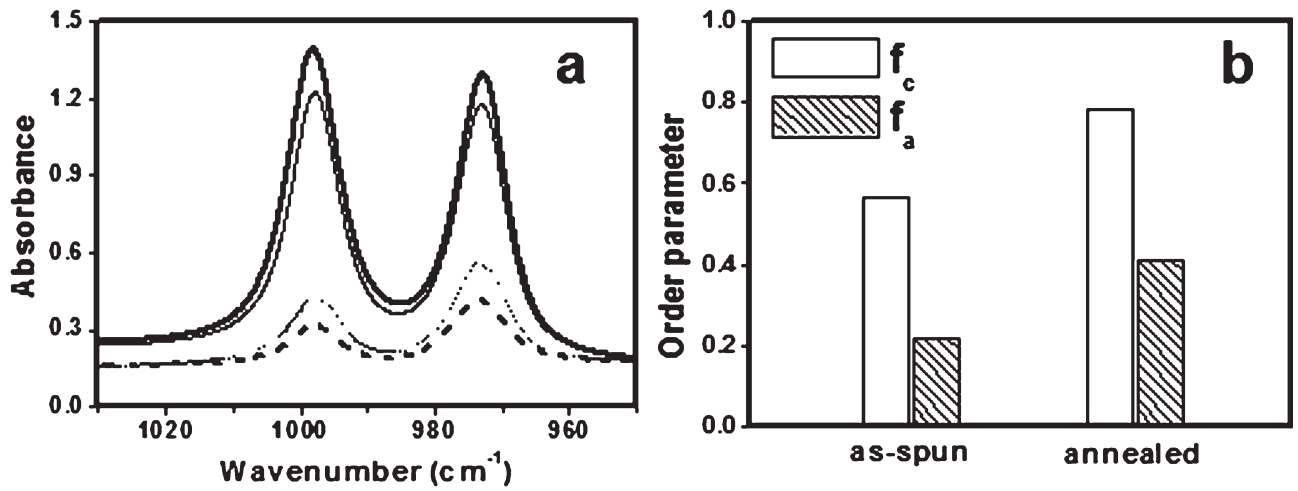

Figure 4 (a) IR spectra, parallel (solid lines) and perpendicular (dashed lines) to the fiber axis, respectively, obtained from as-spun (thin lines) and annealed (thick lines) iPP monofilaments, and (b) the deduced order parameter of the crystalline and amorphous phases.

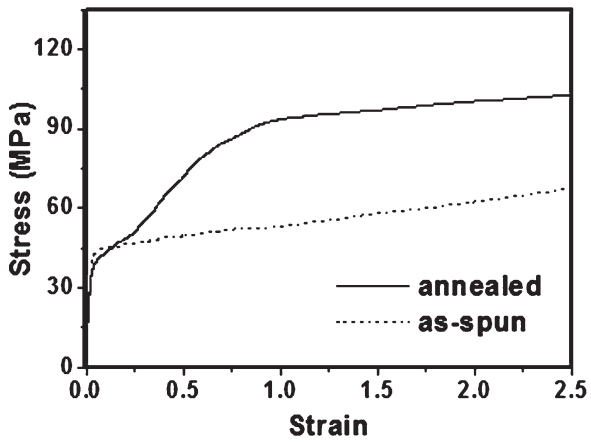

Figure 5 Mechanical responses of as-spun and annealed iPP monofilaments under stretching.

orientation is observed during stretching of as-spun monofilaments. Obviously, the evolution of molecular orientation revealed by the micro-FTIR studies is well correlated with the mechanical responses shown in Figure 5, which gives a deep insight into the relation between structure and mechanical properties of iPP monofilaments.

CONCLUSIONS

Enhanced molecular orientation of both amorphous and crystalline phases in the iPP monofilaments upon annealing around melting peak is unambiguously confirmed by 2D-WAXD and micro-FTIR measurements. It is believed that the recrystallization, nucleated by the surviving oriented crystals, should be responsible for the unusual increase in the molecular orientation. As a consequence, significant strain hardening is presented in the annealed monofilaments with high initial molecular orientation. In addition, the improved stability of crystals in the annealed monofilaments also contributes to the remarkable stress increment before a critical network stress is reached. Once the destruction of crystals sets in, the molecular orientation in the amorphous phase becomes saturated, as confirmed by the micro-FTIR studies of stretching.

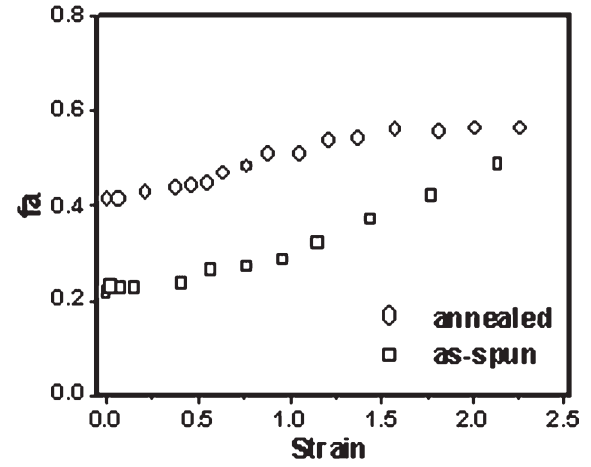

Figure 6 Evolution of order parameters in the amorphous phases during stretching of as-spun and annealed iPP monofilaments.

The authors also thank the NSRL (Hefei, China) for the beam time of 2D-WAXD measurements.

References

1. Arvidson, S. A.; Khan, S. A.; Gorga, R. E. Macromolecules 2010, 43, 2916.
2. Andreassen, E.; Myhre, O. J.; Hinrichsen, E. L.; Grøstad K. J Appl Polym Sci 1994, 52, 1505.
3. Sheehan, W. C.; Cole, T. B. J Appl Polym Sci 1964, 8, 2359.
4. Nadella, H. P.; Henson, H. M.; Spruiell, J. E.; White, J. L. J Appl Polym Sci 1977, 21, 3003.
5. Somani, R. H.; Yang, L.; Hsiao, B. S.; Sun, T.; Pogodina, N. V.; Lustiger, A. Macromolecules 2005, 38, 1244.
6. Dukovski, I.; Muthukumar, M. J Chem Phys 2003, 118, 6648.
7. Na, B.; Wang, Y.; Zhang, Q.; Fu, Q. Polymer 2004, 45, 6245.
8. Stribeck, N.; Nöchel, U.; Camarillo, A. A.; Roth, S. V.; Dommach, M.; Bösecke, P. Macromolecules 2007, 40, 4535.
9. Schimanski, T.; Peijs, T.; Lemstra, P. J.; Loos, J. Macromolecules 2004, 37, 1810.
10. Nadella, H. P.; Spruiell, J. E.; White, J. L. J Appl Polym Sci 1978, 22, 3121.
11. Kish, M. H.; Shoushtari, S. A.; Kazemi, S. Iran Polym J 2000, 9, 239.
12. Foot, J. S.; Ward, I. M. J Mater Sci 1975, 10, 955.
13. Penning, J. P.; van Ruiten, J.; Brouwer, R.; Gabriëlse, W. Polymer 2003, 44, 5869.
14. Botev, M.; Neffati, R.; Rault, J. Polymer 1999, 40, 5227.
15. Garton, A.; Stepaniak, R. F.; Carlsson, D. J.; Wiles, D. M. J Polym Sci Polym Phys Ed 1978, 16, 599.
16. Samuels, R. J. J Polym Sci Polym Phys Ed 1979, 17, 535.
17. Noether, H. D. Prog Colloid Polym Sci 1979, 66, 109.
18. Na, B.; Lv, R. H.; Tian, N. N.; Xu, W. F.; Li, Z. J.; Fu, Q. J Polym Sci Polym Phys 2009, 47, 898.
19. Zhu, P. W.; Edward, G. J Mater Sci 2008, 43, 6459.
20. Sun, X.; Li, H.; Zhang, X.; Wang, J.; Wang, D.; Yan, S. Macromolecules 2006, 39, 1087.
21. Kitayama, T.; Utsumi, S.; Hamada, H.; Nishino, T.; Kikutani, T.; Ito, H. J Appl Polym Sci 2003, 88, 2875.
22. Teckoe, J.; Olley, R. H.; Bassett, D. C. J Mater Sci 1999, 34 2065.
23. Loos, J.; Schimanski, T.; Hofman, J.; Peijs, T.; Lemstra, P. J. Polymer 2001, 42, 3827.
24. Song, Y.; Nemoto, N. Polymer 2005, 46, 6522.
25. Huy, T. A.; Adhikari, R.; Lüpke, T.; Henning, S.; Michler, G. H. J Polym Sci Polym Phys 2004, 42, 4478.
26. Koike, Y.; Cakmak, M. Polymer 2003, 44, 4249.
27. Haward, R. N. Macromolecules 1993, 26, 5860.
28. Men, Y.; Rieger, J.; Strobl, G. Phys Rev Lett 2003, 91, 095502.
29. De Rosa, C.; Auriemma, F.; de Ballesteros, O. R. Phys Rev Lett 2006, 96, 167801.
30. Na, B.; Lv, R. H.; Xu, W. F. J Appl Polym Sci 2009, 113, 4092.
31. Na, B.; Lv, R. H.; Xu, W. F.; Yu, P. S. J Phys Chem B 2007, 111, 13206.
32. Brady, J. M.; Thomas, E. L. J Mater Sci 1989, 24, 3311.